

RESEARCH ARTICLE

Analysis of effects of material anisotropy on ductile damage using microscopic unit-cell model

Sanjeev Koirala  | Steffen Gerke  | Michael Brüning

Institut für Mechanik und Statik,
Universität der Bundeswehr München,
Neubiberg, Germany

Correspondence

Sanjeev Koirala, Institut für Mechanik
und Statik, Universität der Bundeswehr
München, Werner-Heisenberg-Weg 39,
85579 Neubiberg, Germany.
Email: sanjeev.koirala@unibw.de

Funding information

Deutsche Forschungsgemeinschaft,
Grant/Award Number: 394286626

Abstract

It is experimentally observed that the failure in ductile metals is mainly due to the nucleation, growth, and coalescence of micro-voids as well as micro-shear-cracks. Furthermore, plastic anisotropy has significant role in damage and failure behavior of ductile metals. Finite element simulations of unit cell provide a basis to understand different mechanisms on micro-scale, for example, changes in shape and size of single voids and defects as well as localization of plastic strains. This contribution deals with the numerical analysis of unit cell containing spherical void subjected to symmetrical boundary conditions taking material anisotropy into account. Elastic isotropic behavior is described by Hooke's law while Hoffman yield criterion considering the strength-differential effect is used to model the anisotropic plastic behavior. Generalized anisotropic stress invariants, generalized stress triaxiality, and generalized Lode parameter are introduced to characterize the stress state in the anisotropic ductile metal. The effect of plastic anisotropy on the damage behavior of the aluminum alloy EN AW-2017A is studied in detail by performing a series of numerical simulations covering a wide range of stress triaxialities and Lode parameters. Stress triaxiality and Lode parameter are controlled and kept constant during the entire loading process. The numerical results are then used to discuss general mechanisms of damage and failure process in ductile metals.

1 | INTRODUCTION

The numerical modeling of damage and failure behavior of materials used in engineering applications should be precise and realistic to ensure the safety and lifetime of the engineering structures. In reality, it is difficult to have a homogeneous material without the presence of initial voids and inclusions. Furthermore, it is well-established from the experiments, that after loading the initial voids enlarge and they coalesce with the neighboring voids forming larger voids ultimately resulting in the final failure of the structures. For a given constitutive damage model at the macroscale, it is imperative to consider the micro-structural information (different micro-defects and matrix properties) and their evolution. Based on the numerical simulations of a unit-cell containing void, the damage behavior of isotropic ductile materials was studied in detail and the stress-state-dependent parameters of the proposed continuum damage model were identified [1, 2]. The

This is an open access article under the terms of the [Creative Commons Attribution](https://creativecommons.org/licenses/by/4.0/) License, which permits use, distribution and reproduction in any medium, provided the original work is properly cited.

© 2023 The Authors. *Proceedings in Applied Mathematics & Mechanics* published by Wiley-VCH GmbH.

determined parameters were used to numerically simulate the damage behavior using the continuum damage model and were verified with large set of experiments under different loading conditions [3–5].

Similarly, various research groups, for example, Refs. [6–8] have performed finite element simulations of microscopic cells to better understand the damage and failure processes in ductile metals. It was shown that the void growth and coalescence depend on the microstructural and material flow properties. In addition, it was evident that the current stress-state considerably affects damage behavior both on the micro- and macro-level. In all of these studies, the elastic–plastic material behavior was assumed to be isotropic. However, plastic anisotropy is induced in rolled metal sheets due to different manufacturing processes like deep drawing, rolling, or extrusion. The resulted plastic anisotropy also influences the damage and failure processes [9]. Therefore, while modeling the material behavior, it is necessary to take the anisotropy into account. The first quadratic anisotropic yield criterion was developed by Hill48 [10]. After that, different quadratic [11, 12] and nonquadratic anisotropic yield criteria [13, 14] have been proposed. Furthermore, Hoffman [15] introduced anisotropic yield criteria considering the strength-differential (SD) effect.

In the present work, finite element simulations of a unit cell containing a spherical void are carried out taking plastic anisotropy into account. Numerical results then are used to discuss the effect of stress state and loading direction on the damage and failure behavior of ductile metals.

2 | CONSTITUTIVE MODELING

The phenomenological continuum damage model introduced by Brünig [16] describes the inelastic deformations and damage behavior of ductile metals. The kinematics is based on damaged and undamaged configurations whereas, using the second-order damage tensor \mathbf{A}^{da} , different damage mechanisms are adequately characterized. However, plastic behavior was assumed to be only isotropic. This damage model has been enhanced by including plastic anisotropy. Hoffman yield criterion [15] is used to model the anisotropic plastic behavior, which is given as

$$f^{pl} = \mathbf{C} \cdot \bar{\mathbf{T}} + \sqrt{\frac{1}{2} \bar{\mathbf{T}} \cdot \mathbf{D} \bar{\mathbf{T}}} - c = 0 \quad (1)$$

where, $\bar{\mathbf{T}}$ is the effective Kirchhoff stress tensor and \mathbf{C} is the second-order tensor containing the parameters to take the SD effect into account with

$$\begin{bmatrix} C_1 & 0 & 0 \\ C_2 & 0 & 0 \\ C_3 & 0 & 0 \end{bmatrix}.$$

Similarly, \mathbf{D} is the fourth-order tensor, which contains the anisotropic material parameters of the Hoffman yield criterion where the components are

$$\begin{bmatrix} C_4 + C_5 & -C_4 & -C_5 & 0 & 0 & 0 \\ -C_4 & C_4 + C_6 & -C_6 & 0 & 0 & 0 \\ -C_5 & -C_6 & C_5 + C_6 & 0 & 0 & 0 \\ 0 & 0 & 0 & C_7 & 0 & 0 \\ 0 & 0 & 0 & 0 & C_8 & 0 \\ 0 & 0 & 0 & 0 & 0 & C_9 \end{bmatrix}$$

and c denotes the equivalent yield stress of the undamaged material. The stress invariants are newly defined using the Hoffman yield criterion. The determination of elastic and plastic anisotropic parameters can be found in detail in Brünig et al. [17]. The first stress invariant is described as

$$\bar{I}_1^H = \frac{1}{a} \mathbf{C} \cdot \bar{\mathbf{T}} \quad \text{with} \quad a = \frac{1}{3} \text{tr} \mathbf{C} \quad (2)$$

whereas the second and the third deviatoric stress invariants are given by

$$J_2^H = \frac{1}{2} \bar{\mathbf{T}} \cdot \mathbf{D} \bar{\mathbf{T}} \quad (3)$$

and

$$J_3^H = \det(\mathbf{D} \bar{\mathbf{T}}). \quad (4)$$

With the help of these generalized stress invariants, the Hoffman stress triaxiality

$$\bar{\eta}^H = \frac{\bar{I}_1^H}{3\sqrt{3}\bar{J}_2^H} \quad (5)$$

and the Hoffman Lode parameter

$$\bar{L}^H = \frac{-3\sqrt{3}\bar{J}_3^H}{2(J_2^H)^{(3/2)}} \quad (6)$$

are introduced to define the stress state of anisotropic materials. The evolution of plastic strains is given by the flow rule

$$\dot{\mathbf{H}}^{pl} = \dot{\gamma} \bar{\mathbf{N}} \quad (7)$$

where $\dot{\gamma}$ represents the equivalent plastic strain rate and $\bar{\mathbf{N}}$ is the normalized deviatoric effective stress tensor defined as

$$\bar{\mathbf{N}} = \frac{\mathbf{D} \bar{\mathbf{T}}}{\|\mathbf{D} \bar{\mathbf{T}}\|}. \quad (8)$$

Similarly, the onset of damage is modeled using the damage criterion

$$f^{da} = \alpha I_1^H + \beta \sqrt{J_2^H} - \sigma = 0 \quad (9)$$

where I_1^H and J_2^H are the generalized stress invariants defined with respect to damaged configurations and σ is the equivalent damage stress. α and β are stress-state- and loading-direction-dependent parameters, which have been identified using an experimental and numerical procedure as in Brünig et al. [17]. Furthermore, the evolution of the damage strains is given by the damage rule as

$$\dot{\mathbf{H}}^{da} = \dot{\mu} \left(\frac{\tilde{\alpha}}{\sqrt{3}} \mathbf{1} + \tilde{\beta} \bar{\mathbf{N}} \right) \quad (10)$$

where $\tilde{\alpha}$ and $\tilde{\beta}$ are scalar parameters dependent on the stress-state and loading direction. $\bar{\mathbf{N}}$ is the normalized deviatoric effective stress tensor with respect to damaged configuration and given as

$$\bar{\mathbf{N}} = \frac{\mathbf{D} \mathbf{T}}{\|\mathbf{D} \mathbf{T}\|} \quad (11)$$

where \mathbf{T} is the Kirchhoff stress tensor.

3 | NUMERICAL SIMULATIONS OF THE UNIT CELL

A finite element model of one eighth of a representative volume element (RVE) containing a spherical void with an initial void volume fraction of 3% is shown in Figure 1.

The numerical simulations are performed using ANSYS (2018), enhanced by user-defined material subroutine (Usermat). Solid 185 type of elements are used with the symmetrical boundary condition considering the regular distribution of micro-defects, while the stress triaxiality and Lode parameter are kept constant during the loading process. In previous

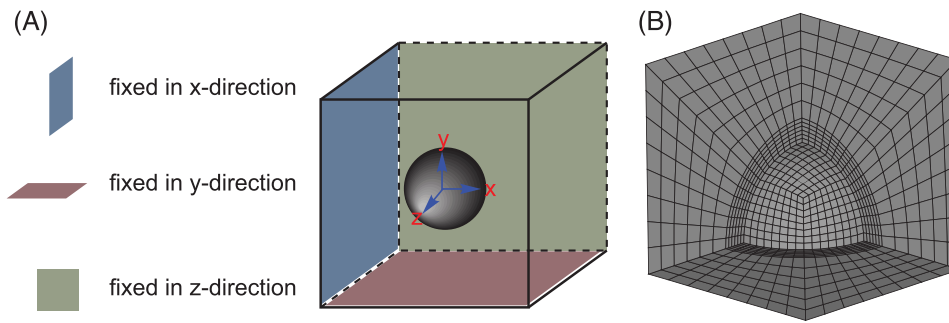


FIGURE 1 (A) Boundary conditions for the unit cell and (B) cut view for one eighth of the unit cell.

studies [1, 2], different shape and size of voids with different initial porosity were numerically studied in detail. It was shown that spherical-shaped void with 3% initial porosity lead to the good approximation for the determination of the state-state-dependent parameters $\tilde{\alpha}$ and $\tilde{\beta}$. Therefore, in this study, only a spherical void with 3% initial void volume fraction is considered. Symmetrical boundary conditions are used as shown in Figure 1A, where the yz -surface, xz -surface, and xy -surface of the unit cell containing an initial void, as marked with different colors are fixed in x -, y -, and z -directions, respectively. The deformation behavior of matrix material is described with the constitutive modeling as given in Section 2, where only elastic–plastic deformations take place. The changes in size and shape of the spherical void give us the damage strains. According to the considered kinematics of the continuum damage model, the total strain rate tensor $\dot{\mathbf{H}}^{RVE}$ in the principal directions (i) is additively decomposed into the elastic $\dot{\mathbf{H}}^{el}$, the effective plastic $\dot{\mathbf{H}}^{pl}$ and the damage part $\dot{\mathbf{H}}^{da}$ as

$$\dot{H}_{(i)}^{RVE} = \dot{H}_{(i)}^{el} + \dot{H}_{(i)}^{pl} + \dot{H}_{(i)}^{da}. \quad (12)$$

Furthermore, the macroscopic elastic–plastic strain rates are given as

$$\dot{\mathbf{H}}^{ep} = \dot{\mathbf{H}}^{el} + \dot{\mathbf{H}}^{pl} = \frac{1}{V} \int_{V_{matrix}} (\dot{\mathbf{h}}^{el} + \dot{\mathbf{h}}^{pl}) dv \quad (13)$$

where $\dot{\mathbf{h}}^{el}$ and $\dot{\mathbf{h}}^{pl}$ are the elastic and plastic strain rates of the matrix material on the micro-level, V represents the current volume of the unit cell, and V_{matrix} indicates the current volume of the matrix material (solid elements). Using Equations (12) and (13), the principal values of the damage strain rate tensor in the macro-level are given by

$$\dot{H}_{(i)}^{da} = \dot{H}_{(i)}^{RVE} - \dot{H}_{(i)}^{ep}. \quad (14)$$

This leads to the principal components of the damage strain tensor as

$$A_{(i)}^{da} = \int \dot{H}_{(i)}^{da} dt. \quad (15)$$

The void volume fraction f is determined using

$$f = \frac{V - V_{matrix}}{V}. \quad (16)$$

In addition, the equivalent strain rate is defined as

$$\dot{\varepsilon}_{eq} = \sqrt{\frac{2}{3} \dot{\mathbf{H}} \cdot \dot{\mathbf{H}}} \quad (17)$$

which is then used to calculate the equivalent strain given by

$$\varepsilon_{eq} = \int \dot{\varepsilon}_{eq} dt. \quad (18)$$

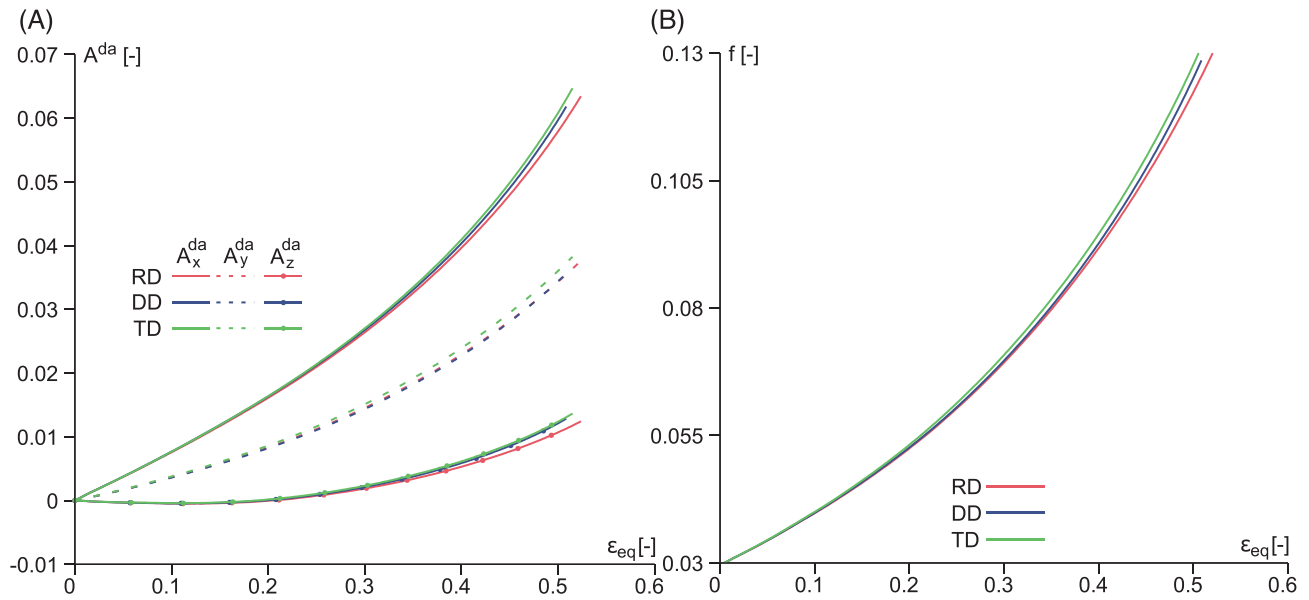


FIGURE 2 (A) Evolution of the damage strain tensor for $\eta^H = 0.75$ and $L^H = 0.23$, (B) evolution of void volume fraction for $\eta^H = 0.75$ and $L^H = 0.23$.

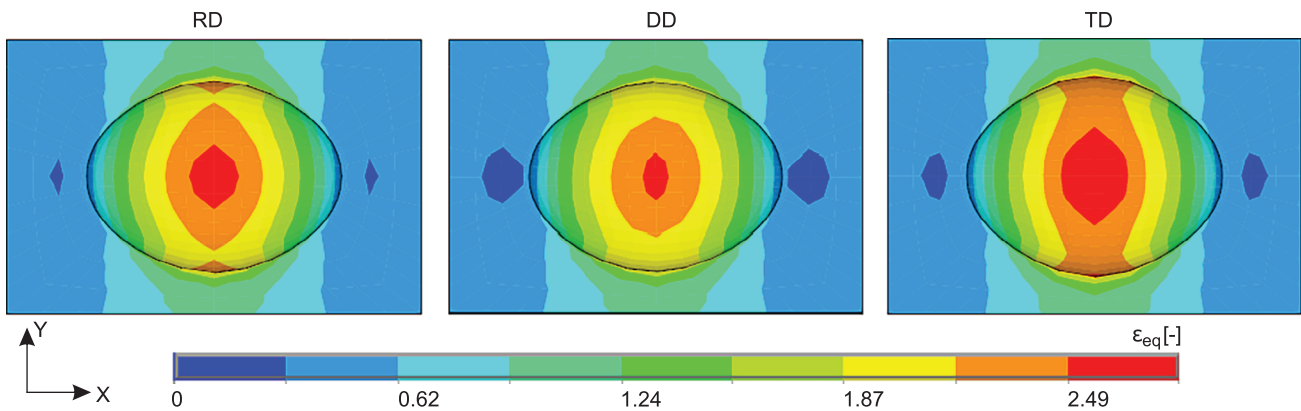


FIGURE 3 Distribution of equivalent strain on one half of the unit cell for $\eta^H = 0.75$ and $L^H = 0.23$.

4 | NUMERICAL RESULTS

Numerical simulations are carried out for different loading ratios $F_x/F_y/F_z$, which result in different stress-states of the RVE. Furthermore, the RVE is loaded in different directions, namely in rolling direction (RD), diagonal direction (DD), and transverse direction (TD), with respect to the RD. Hence, taking material anisotropy into account, the damage behavior of unit cell covering wide range of stress triaxialities is analyzed in detail. But, in this work, only the results for two loading ratios are discussed. The evolution of damage strains for the loading ratio $F_x/F_y/F_z = 1/0.63/0.27$ is shown in Figure 2A. All of the damage strains increase, x -components of damage strain for all RDs are higher as compared to y and z -components. A_x^{da} for RD reaches to 0.065 while all of the A_z^{da} components are nearly equal to 1%. There is only a slight difference in the evolution of damage strains after ϵ_{eq} attains 35%. The Hoffman stress triaxiality $\eta^H = 0.75$ and the Hoffman Lode parameter $L^H = 0.23$, indicating the presence of high hydrostatic stress state where the damage process is governed mainly by void growth and coalescence. This phenomenon can be seen in Brünig et al. [9], where for the similar stress state, pictures of fracture surface were taken using scanning electron microscopy. Similarly, the void volume fraction in Figure 2B increases rapidly for all loading directions while only a minimum difference is seen in f once when ϵ_{eq} equals 40%. The local distribution of ϵ_{eq} on the elements is given in Figure 3. The initial spherical void deforms to become ellipsoid and there are no significant differences in the value of ϵ_{eq} among the three different loading directions.

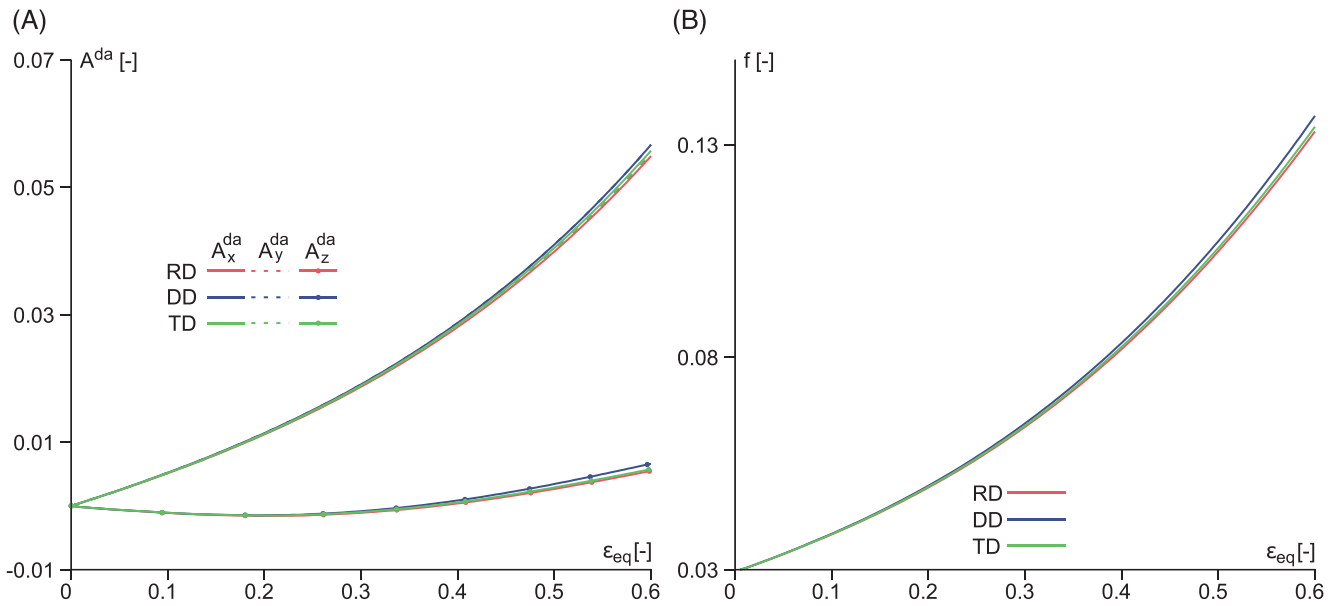


FIGURE 4 (A) Evolution of damage strain tensor for $\eta^H = 0.65$ and $L^H = 1$, (B) evolution of void volume fraction for $\eta^H = 0.65$ and $L^H = 1$.

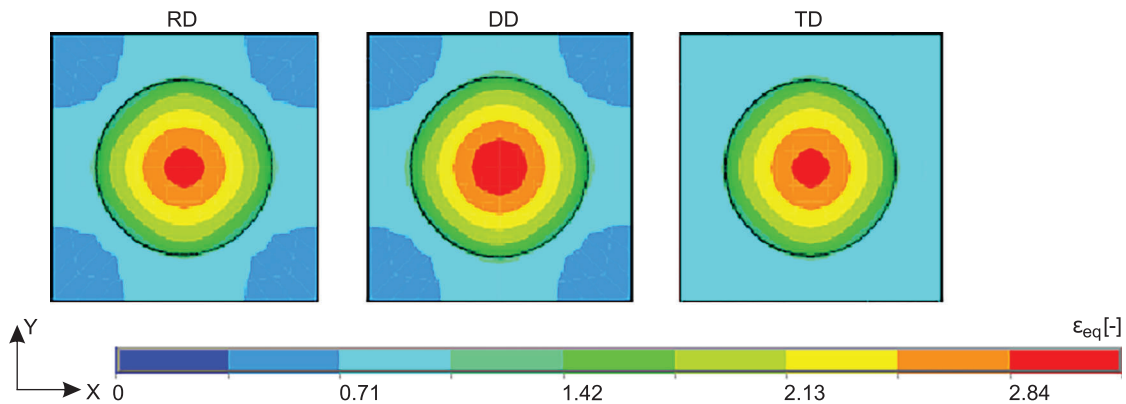


FIGURE 5 Distribution of equivalent strain on one half of the unit cell for $\eta^H = 0.65$ and $L^H = 1$.

Furthermore, for the loading ratio $F_x/F_y/F_z = 1/1/0.25$, damage strain formation is shown in Figure 4A. The stress-state parameters η^H and L^H are 0.65 and 1, respectively. A_x^{da} for RD, DD, and TD is almost equal and goes up to 0.0582 while A_z^{da} for all loading directions reaches up to 0.0052. In addition, in Figure 4B, the porosity at the beginning for all the three loading directions is similar, but varies slightly once the ϵ_{eq} becomes around 35%. The distribution of equivalent strain is depicted in Figure 5. The spherical void does not change in shape but does change in size. Again, only small but no remarkable differences can be seen in ϵ_{eq} value amid the loading directions.

5 | CONCLUSIONS

In this paper, finite element analysis to identify the effect of plastic anisotropy on damage evolution on the micro-level is performed. For that purpose, numerical simulations using unit cell containing a spherical void located at the center of the RVE have been performed, especially for high stress triaxialities. Assuming that the material displays a regular porous microstructure, symmetrical boundary conditions are used and the stress triaxiality and Lode parameter are enforced to be constant during the loading. Hoffman yield criterion is used to model the plastic anisotropic behavior. Generalized stress invariants for the anisotropic ductile metal based on the Hoffman yield criterion are used to characterize the stress state. After certain equivalent strain, small differences can be seen in the evolution of damage strains between RD, DD, and TD.

Similar trend can be observed for the void volume fraction. Equivalent plastic strain distribution on the element level is also not the same for three different loading directions. Therefore, the effect of the stress state and the loading direction on damage behavior has to be considered in continuum damage model. Also, it is difficult to experimentally study the damage and failure processes on the micro-level, for example, a RVE containing voids and inclusions, and their effect on the macro-level. Performing the numerical simulations for wide range of stress triaxiality, different damage parameters can be identified for the proposed damage rule. Therefore, the numerical simulations performed using RVE in this work can be considered as quasi-experimental and the results can be used to validate the proposed phenomenological continuum damage model.

ACKNOWLEDGMENTS

The authors gratefully acknowledge financial support of the Deutsche Forschungsgemeinschaft (DFG, German Research Foundation)—project number 394286626.

Open access funding enabled and organized by Projekt DEAL.

ORCID

Sanjeev Koirala  <https://orcid.org/0000-0002-2146-5099>

Steffen Gerke  <https://orcid.org/0000-0003-2261-3855>

REFERENCES

1. Brünig, M., Gerke, S., & Hagenbrock, V. (2013). Micro-mechanical studies on the effect of the stress triaxiality and the lode parameter on ductile damage. *International Journal of Plasticity*, *50*, 49–65.
2. Brünig, M., Gerke, S., & Hagenbrock, V. (2014). Stress-state-dependence of damage strain rate tensors caused by growth and coalescence of micro-defects. *International Journal of Plasticity*, *63*, 49–63.
3. Wei, Z., Zistl, M., Gerke, S., & Brünig, M. (2022). Analysis of ductile damage and fracture under reverse loading. *International Journal of Mechanical Sciences*, *228*, 107476.
4. Wei, Z., Zistl, M., Gerke, S., & Brünig, M. (2023). Analysis of ductile damage evolution and failure mechanisms due to reverse loading conditions for the aluminum alloy EN-AW 6082-T6. *PAMM*, *23*, e202200012.
5. Wei, Z., Gerke, S., & Brünig, M. (2023). Damage and fracture behavior under non-proportional biaxial reverse loading in ductile metals: Experiments and material modeling. *International Journal of Plasticity*, *171*, 103774.
6. McClintock, F. A. (1968). A criterion for ductile fracture by the growth of holes. *Journal of Applied Mechanics*, *35*(2), 363–371.
7. Gao, X., & Kim, J. (2006). Modeling of ductile fracture: significance of void coalescence. *International Journal of Solids and Structures*, *43*(20), 6277–6293.
8. Scheyvaerts, F., Onck, P. R., Tekoğlu, C., & Pardoën, T. (2011). The growth and coalescence of ellipsoidal voids in plane strain under combined shear and tension. *Journal of the Mechanics and Physics of Solids*, *59*(2), 373–397.
9. Brünig, M., Koirala, S., & Gerke, S. (2022). Analysis of damage and failure in anisotropic ductile metals based on biaxial experiments with the H-specimen. *Experimental Mechanics*, *62*, 183–197.
10. Hill, R. (1948). A theory of the yielding and plastic flow of anisotropic metals. *Proceedings of the Royal Society of London. Series A. Mathematical and Physical Sciences*, *193*(1033), 281–297.
11. Stoughton, T. B., & Yoon, J. W. (2009). Anisotropic hardening and non-associated flow in proportional loading of sheet metals. *International Journal of Plasticity*, *25*(9), 1777–1817.
12. Hill, R. (1990). Constitutive modelling of orthotropic plasticity in sheet metals. *Journal of the Mechanics and Physics of Solids*, *38*(3), 405–417.
13. Barlat, F., Aretz, H., Yoon, J. W., Karabin, M. E., Brem, J. C., & Dick, R. E. (2005). Linear transformation-based anisotropic yield functions. *International Journal of Plasticity*, *21*(5), 1009–1039.
14. Bron, F., & Besson, J. (2004). A yield function for anisotropic materials application to aluminum alloys. *International Journal of Plasticity*, *20*(4–5), 937–963.
15. Hoffman, O. (1967). The brittle strength of orthotropic materials. *Journal of Composite Materials*, *1*(2), 200–206.
16. Brünig, M. (2003). An anisotropic ductile damage model based on irreversible thermodynamics. *International Journal of Plasticity*, *19*(10), 1679–1713.
17. Brünig, M., Koirala, S., & Gerke, S. (2023). A stress-state-dependent damage criterion for metals with plastic anisotropy. *International Journal of Damage Mechanics*, *32*, 811–832.

How to cite this article: Koirala, S., Gerke, S., & Brünig, M. (2023). Analysis of effects of material anisotropy on ductile damage using microscopic unit-cell model. *Proceedings in Applied Mathematics and Mechanics*, e202300046. <https://doi.org/10.1002/pamm.202300046>